Magnetic chaos healing in the helical reversed-field pinch: indications from the volume-preserving field line tracing code NEMATO

Journal of Physics: Conference Series **260** (2010) 012003 doi:10.1088/1742-6596/260/1/012003

Magnetic chaos healing in the helical reversed-field pinch: indications from the volume-preserving field line tracing code NEMATO

D Bonfiglio[1], M Veranda[1], S Cappello[1], L Chacón[2] and G Spizzo[1]

[1] Consorzio RFX, Euratom-ENEA Association, Padova, Italy
[2] Oak Ridge National Laboratory, Oak Ridge, Tennessee, USA

E-mail: daniele.bonfiglio@igi.cnr.it

Abstract. The emergence of a self-organized reversed-field pinch (RFP) helical regime, first shown by 3D MHD numerical simulations, has been highlighted in the RFX-mod experiment at high current operation (I_P above 1 MA). In fact, a quasi-stationary helical configuration spontaneously appears, characterized by strong internal electron transport barriers. In such regime electron temperature and density become, to a very good approximation, functions of the helical flux coordinate related to the dominant helical magnetic component. In addition, this regime is diagnosed to be associated with the topological transition to a single-helical-axis (SHAx) state, achieved after the expulsion of the separatrix of the dominant mode's magnetic island. The SHAx state is theoretically predicted to be resilient to the magnetic chaos induced by secondary modes. In this paper, we present initial results of the volume-preserving field line tracing code NEMATO [Finn J M and Chacón L 2005 *Phys. Plasmas* **12** 054503] applied to study the magnetic topology resulting from 3D MHD simulations of the RFP. First, a successful 2D verification test of the code is shown, then, initial application to a systematic study of chaos healing in the helical RFP is discussed. The separatrix disappearance is confirmed to play an essential role for chaos healing. The triggering effect of a reversed magnetic shear for the formation of ordered surfaces within magnetic chaos is also diagnosed.

1. Introduction

The reversed-field pinch (RFP) is a toroidal magnetic configuration for plasma confinement. Similarly to what occurs in the tokamak, RFP plasmas are obtained by driving a toroidal current in a plasma embedded in a toroidal magnetic field. However, the plasma current in the RFP is strong enough with respect to the toroidal flux to drive a significant helical shaping of the plasma column. This deformation is related to one or more resistive kink-tearing instabilities which nonlinearly saturate at finite amplitude with the help of the toroidal field reversal at the plasma edge, whence comes the name of the configuration. In the multiple helicity (MH) regime, characterized by the presence of many magnetic fluctuations, plasma confinement is degraded by stochastic transport due to the overlap of core magnetic islands, and only an edge confinement region survives. The turbulent MH state was the first to be studied in RFP devices. During the last years, however, a tendency to develop a regime characterized by a good degree of helical symmetry has been observed in different RFP experiments when the plasma current is increased [1]. The first obtained quasi-single helicity (QSH) regime was characterized by the appearance of a thermal helical structure corresponding to the O-point of the magnetic island associated with

the dominant helical mode. Recently, during high current operation (up to 1.7 MA) in the RFX-mod experiment, a quasi-stationary QSH state with a strong internal transport barrier (ITB) enclosing a broad hot core (with electron temperature above 1 keV) spontaneously appeared [2]. In such regime electron temperature, density, and soft X-ray emissivity become, to a very good approximation, functions of the helical flux coordinate related to the dominant mode. This is observed together with the decrease of the secondary modes amplitude, and shows that the high current QSH regime in RFX-mod is close to a single helicity (SH) state.

Many features of the experimental RFP phenomenology have been first shown by theory and numerical modelling. Three-dimensional (3D) visco-resistive magnetohydrodynamic (MHD) numerical simulations of the RFP reproduce quite well the qualitative magnetic behaviour of experimental MH and QSH regimes [3, 4] and shows the existence of pure SH equilibrium solutions [5, 6] which spontaneously appear when the visco-resistive dissipation is increased [7, 4]. As far as transport in concerned, the edge confinement in the MH state has been associated with the presence of a $m = 0$ magnetic islands chain at the field reversal radius [8]. Regarding the QSH regime, chaos healing is theoretically predicted to be induced by the expulsion of the separatrix of the dominant mode's magnetic island [9], corresponding (as described in this paper) to the topological transition from a double-axis (DAx) to a single-helical-axis (SHAx) state. The same transition is diagnosed to occur in the high current QSH regime of RFX-mod [2]. The increased resilience to magnetic chaos predicted for the SHAx state could therefore be related with the good confinement properties of that experimental state, namely the presence of a hot helical core surrounded by an ITB. Similarly to what happens in the tokamak, a null of the magnetic shear could also help to reduce transport at the ITB. In fact, the location of the core transport barrier in RFX-mod is found to be well correlated with the maximum of the non monotonic q profile typical of the SHAx regime [10, 11]. A sheared plasma flow is a possible player for the ITB sustainment [12] against the microturbulence which could arise at the barrier [13].

In this paper, we present an initial application to the study of the conditions for chaos healing in the helical RFP, performed with the volume-preserving field line tracing code NEMATO [14]. The code is used to compute the topology of the magnetic field in a periodic cylinder provided by numerical simulations with the 3D nonlinear visco-resistive MHD code SPECYL [4]. The paper is organized as follows. The features of NEMATO are described in Sec. 2. The verification benchmark of the code against magnetic fields with either helical or poloidal symmetry is reported in Sec. 3. The application of NEMATO to a QSH simulation with separatrix disappearance is discussed in Sec. 4. It is observed that the chaos induced by secondary modes is cured in a short time around the transition to the SHAx state. The role played by the separatrix expulsion is thus confirmed. In addition, the formation of the first conserved surfaces within the chaotic region is shown to occur where the magnetic shear is reversed. As remarked in Sec. 5, the present work will be extended to more general cases of quasi-single helicity RFP states.

2. The field line tracing code NEMATO

The field line tracing code NEMATO is a volume-preserving integrator for solenoidal fields on a (cylindrical or toroidal) 3D grid [14]. It solves the magnetic field line equation $\frac{\mathrm{d}\mathbf{x}}{\mathrm{d}\tau} = \mathbf{B}(\mathbf{x})$, where $\mathbf{B}$ is the magnetic field given on the 3D grid $\mathbf{x}$ and the "time" τ represents a coordinate along the field line. The two main features of the code are the interpolation scheme, which ensures the solenoidal nature of the field everywhere in the domain, and the volume-preserving integration scheme. Together, they exactly preserve $\nabla \cdot \mathbf{B} = 0$ to numerical round-off along each magnetic field line. As a result, integrable and chaotic field lines are distinguished well one from each other. This makes the code particularly suitable to study weakly chaotic magnetic fields typical of the quasi-single helicity RFP, and represents a novelty with respect to other field-line tracing tools used in past studies [9]. A non volume-preserving version of NEMATO, based on the high-order, adaptive LSODE library [15], is also available for fast preliminary analysis.

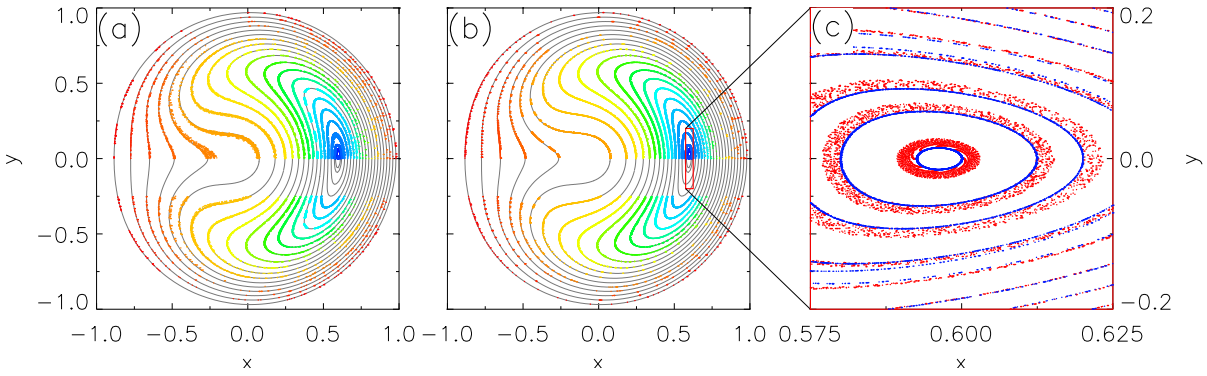

Figure 1. Verification of NEMATO against RFP configurations with helical symmetry provided by the MHD code SPECYL. Poincaré maps on the $z = 0$ plane (colored dots) are compared with the helical flux function χ (black contours levels). Results obtained with a grid resolution of $100 \times 256 \times 256$ and $100 \times 256 \times 2048$ radial $\times$ azimuthal $\times$ axial points are reported in panel (a) and (b), respectively. To make the comparison easier, intersections of the field lines with the Poincaré surface in the $-0.25 \leq y \leq 0$ band are not shown. A blow-up of the most resolved simulation in the region around the helical axis is shown in panel (c), together with the result of the non volume-preserving version of NEMATO with the same resolution (red dots).

3. Verification benchmark against symmetric magnetic fields

If a magnetic field is characterized by a two-dimensional (2D) symmetry, magnetic field lines are integrable in the whole field domain, i.e., they trace out well defined magnetic surfaces. The verification of NEMATO has been performed on the basis of this principle. The code has been run on 2D symmetric magnetic fields provided by the MHD code SPECYL, and it has been checked that magnetic field lines integrated by NEMATO (without any assumption about the magnetic field symmetry) lie on the isosurfaces of the flux function ρ computed from the definition $\mathbf{B} \cdot \nabla \rho = 0$. The verification benchmark has been performed by considering magnetic fields with either helical or poloidal symmetry.

SPECYL solves the MHD equations in a periodic cylinder (rectified torus) with radial coordinate r, azimuthal (poloidal) coordinate θ and axial (toroidal) coordinate z with a period of $2\pi R_0$. The aspect ratio of the rectified torus is set to $R_0 = 4$. In helical symmetry, all quantities depend on the two variables r and $u = m\theta - \frac{n}{R_0} z$, where m and n are the poloidal and toroidal mode numbers, respectively. The helical flux function χ such that $\mathbf{B} \cdot \nabla \chi = 0$ is defined by $\chi(r, u) = m A_z + \frac{n}{R_0} r A_\theta$, where A_z and A_θ are the toroidal and the poloidal components of the vector potential $\mathbf{A}$. For the verification benchmark with NEMATO, we have employed a single helicity RFP equilibrium obtained as the nonlinear saturation state of a resistive kink-tearing instability with $m = 1$, $n = -10$. As reported in the Poincaré maps of Figs. 1(a) and 1(b), results depend on the 3D grid resolution. When a resolution of 100 radial $\times$ 256 azimuthal $\times$ 256 axial grid points is employed, the matching between the field line trajectories and the helical flux surfaces is reasonable, but a certain drift of the field lines away from their initial magnetic surface is observed. This drift is due to the number of mesh points in the axial direction, which is not enough to adequately sample the helical field with its high toroidal mode number $n = -10$. When the grid resolution is increased to $100 \times 256 \times 2048$ points, the drift disappears and the matching of field lines with helical flux surfaces is quite good. The latter grid resolution is hence employed in the remainder of the paper. The volume-preserving scheme employed by NEMATO can be appreciated by comparing it with the non volume-preserving version of the code, as shown in the blow-up of Fig. 1(c). For the same length of the field line integration, NEMATO orbits

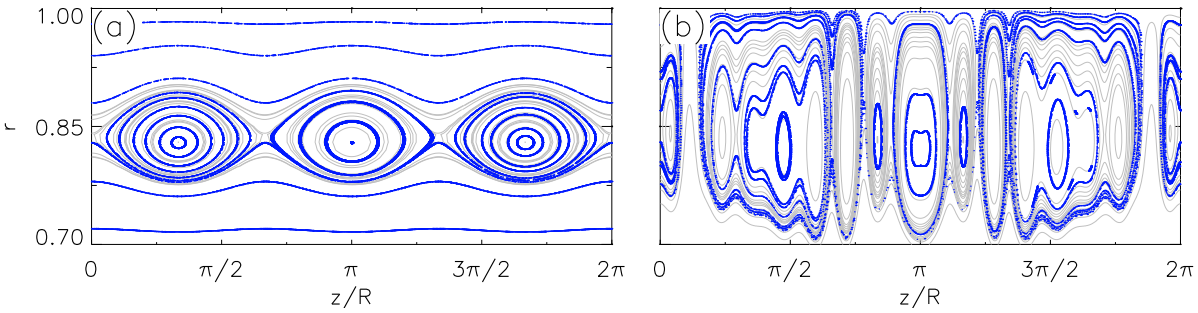

Figure 2. Verification benchmark of NEMATO against RFP configurations with poloidal symmetry provided by the MHD code SPECYL. Poincaré maps on the $\theta = 0$ plane (colored dots) are compared with the toroidal flux function Φ (gray contours levels). The $m = 0$ modes taken into account are (a) the $n = 3$ mode only and (b) all the $1 \leq n \leq 25$ modes involved in the MHD computation.

are perfectly defined, while drifts are produced by the non volume-preserving code, even when the best grid resolution is employed. NEMATO has also been benchmarked against magnetic configurations with poloidal symmetry, obtained from a 3D multiple helicity RFP simulation when $m = 0$ modes only are supplied to the field line tracing code. As reported in Fig. 2, magnetic field lines computed by NEMATO trace out clearly defined magnetic surfaces, like in the case of helical symmetry. These magnetic surfaces match very well with the contour levels of the toroidal flux function $\Phi(r, z) = rA_\theta$ such that $\mathbf{B} \cdot \nabla\Phi = 0$.

4. Study of the chaos healing effect in the helical RFP

As an initial application to the study of chaos healing in the QSH, we consider a 3D MHD simulation with a full spectrum of allowed MHD modes with $0 \leq m \leq 4$ and two helical perturbations of the initial axis-symmetric equilibrium, corresponding to the unstable $m = 1$ modes with $n = -9$ and $n = -10$. The Lundquist and Prandtl numbers are set to $S = 3 \times 10^4$ and $P = 10^3$, respectively. Details of the MHD simulation are reported in Fig. 3. The $n = -9$ mode, the most unstable between the two perturbed modes, is the dominant mode in the second part of the linear growth phase and at the beginning of the nonlinear saturation phase, when the other $m = 1$ modes arise. The nonlinear dynamics makes the $n = -10$ mode to become the dominant one after $t = 2000\ \tau_A$. The exponential decay of the secondary modes brings the system to the final $n = -10$ SH equilibrium configuration. In this study, we focus our attention to the time window where the $n = -9$ mode is the dominant one. The contour levels of the helical flux function χ computed by assuming a $n = -9$ helical symmetry are plotted, for five selected simulation times, in Fig. 3(b). The first two times are characterized by the DAx magnetic topology. In fact, the magnetic field displays two magnetic axes: the unperturbed axis-symmetric one and the one related to the O-point of the $n = -9$ magnetic island. Flux surfaces winding around the two axes are kept apart by the separatrix of the magnetic island, whose width is growing in time. Just before $t = 750\ \tau_A$, a topological transition to the SHAx state occurs: the magnetic separatrix disappears after the coalescence of the axis-symmetric O-point with the island X-point, and the island O-point becomes the only (helical) magnetic axis, as shown for the last three times. For every flux surface which encloses the helical axis we have computed (again by assuming $n = -9$ helical symmetry) the safety factor defined as $q(\chi) = \frac{\mathrm{d}\Phi(\chi)}{\mathrm{d}\psi(\chi)}$, where $\Phi(\chi)$ and $\psi(\chi)$ are, respectively, the toroidal and poloidal flux across the helical flux surface χ. The safety factor $q(\chi)$ gives the number of toroidal turns field lines

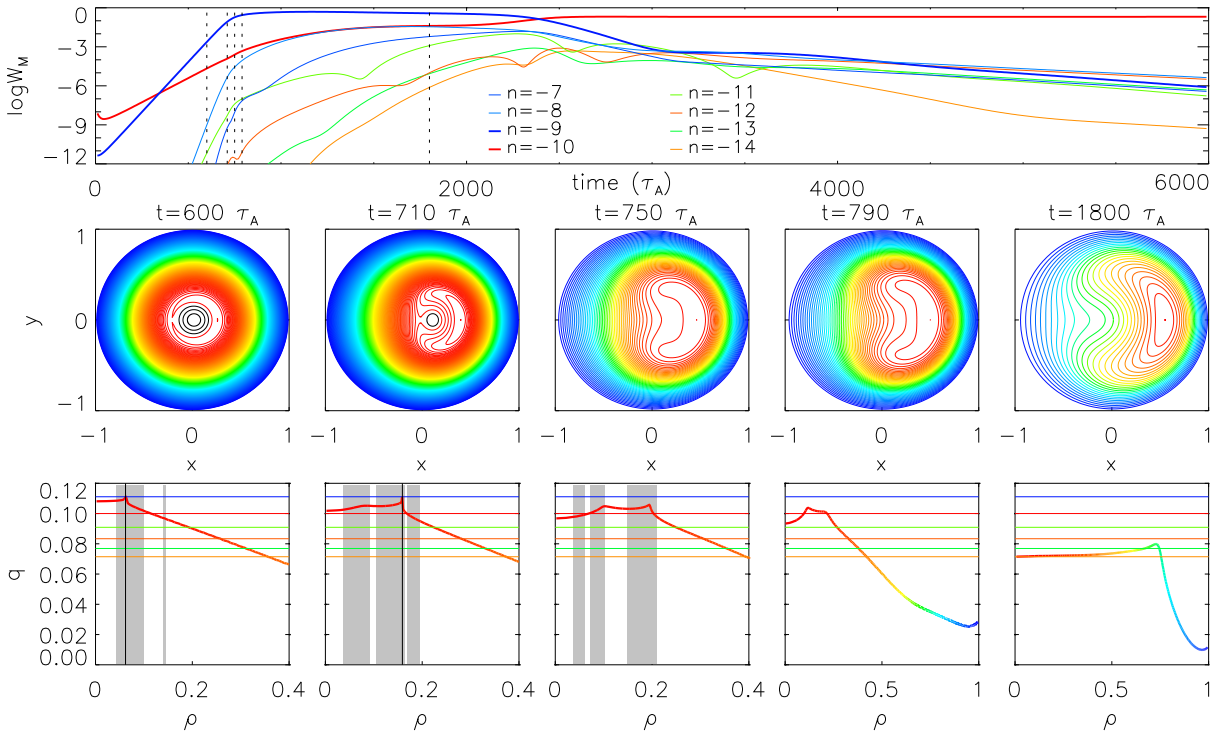

Figure 3. SPECYL simulation employed for the NEMATO study of the chaos healing effect in the RFP. The temporal evolution of the magnetic energy of the main $m = 1$ modes is reported in panel (a). The simulation times chosen for the analysis with NEMATO are marked with dashed vertical lines. For these times, we report (b) the contour levels of the helical flux function χ and (c) the q profile as a function of the effective radius ρ. Both χ and q are computed by assuming $n = -9$ helical symmetry. The color of the flux surfaces in panel (b) refer to their ρ values and reflect the color shifts in the q profiles of panel (c). The ρ value corresponding to the separatrix is marked in panel (c) with a black vertical line, while shaded vertical bands refer to chaotic regions in the Poincaré plots of Fig. 4. The $m = 1$ rational values with n from $n = -9$ to $n = -14$ are shown with horizontal lines with the same color code employed in panel (a).

perform for one poloidal turn *around the helical axis* and is introduced here for the intepretation of the magnetic field topology, as discussed below. The q profile for the selected times is shown in Fig. 3(c) as a function of the effective radius $\rho = (\chi/\chi_b)^{1/2}$, where χ_b is the helical flux at the plasma boundary and $\chi = 0$ at the helical axis. As derived in the framework of the Hamiltonian representation of the magnetic field [16], $q \to 1/9$ at the separatrix. $q(0)$, the safety factor at the helical axis, is close to $1/9$ at $t = 600\ \tau_A$ and decreases in time as the magnetic island width increases. At $t = 710\ \tau_A$, an additional maximum of q appears inside the separatrix. Just after the separatrix expulsion, $t = 750\ \tau_A$, there is still a peak at the "separatrix ghost" but its value is below $1/9$. The hollow between the two q maxima is now more pronounced. In addition, $q(0) < 1/10$, meaning that a second resonance for the $m = 1$, $n = -10$ mode is present. At $t = 790\ \tau_A$, the peak at the separatrix ghost is more depressed. Later in time, at $t = 1800\ \tau_A$, the q profile is much lower and it takes the same non-monotonic shape as reported in Refs. [10, 11] (we note that the maximum of q does not come from the separatrix ghost).

We now discuss the topology of the magnetic field at the five selected times, as computed by NEMATO. The corresponding Poincaré plots on the $z = 0$ and $\theta = 0$ surfaces of section are reported in Fig. 4. At $t = 600\ \tau_A$, the $n = -9$ and $n = -10$ island chains produced by the

two perturbed modes are clearly visible along the z direction in the $\theta = 0$ plane. The $n = -10$ island chain is distorted by the $n = -9$ helical perturbation. By overplotting the $n = -10$ conserved surfaces on the $n = -9$ helical flux surfaces of Fig 3(b), it could be shown that they lie on the helical flux surface with $q(\chi) = 1/10$. The separatrices of the two magnetic islands (computed from the helical flux functions with the two related helicities) overlap. According to the Chirikov overlap criterion [17], magnetic chaos develops in the region between the two islands and, in particular, inside the separatrix of the $n = -9$ mode. The magnetic surfaces close to the cylindrical axis remain perfectly conserved, as well as those located in the outer region. Secondary islands due to the beat of the two main islands are also visible inside the chaotic sea. As for the $n = -10$ island, the effective radial positions of the secondary islands with respect to the helical axis correspond to helical flux surfaces with rational q values. As time increases, the chaotic volume inside the separatrix of the $n = -9$ island increases together with the island width. At $t = 710\ \tau_A$, when the strongly deformed $n = -10$ island chain is quite narrow but still visible just outside the $n = -9$ separatrix, a broad chaotic region is observed between the remnant conserved surfaces around the helical axis and those around the (helically displaced) "cylindrical" axis. However, a region with conserved surfaces appears in the middle of the chaotic region. The ρ position of the conserved layer corresponds to the region with negative magnetic shear between the maximum of q inside the separatrix and the separatrix itself, as marked by means of an unshaded band in Fig. 3(c). The extent of the conserved layer increases in time with the deepening of the q hollow. In the meantime, the separatrix expulsion occurs, which is seen by disappearance of the helical axis at $t = 750\ \tau_A$. At this time, the conserved layer is rather large. Again, it turns out to be located in the $\frac{\mathrm{d}q}{\mathrm{d}\rho} \leq 0$ region of the q profile. Since $q(0)$ is below $1/10$, a $m = 1$, $n = -10$ island chain appears inside the chaotic region at the $q = 1/10$ resonant surface close to the helical axis [18]. Conserved surfaces corresponding to the original $n = -10$ island are not found at this time. At $t = 790\ \tau_A$, when the separatrix is well expulsed, chaos is strongly reduced in the whole domain. It only survives at the separatrix of the outer $n = -10$ island, which reappears with a rather elongated shape at this time. The chaos healing effect is robust and lasts for a long time, even if the amplitude of secondary modes is increasing. At $t = 1800\ \tau_A$, for instance, well defined magnetic surfaces are still observed in the whole domain, either closed around the helical axis or in the form of secondary islands, now with $n = -14$ due to the lower q profile.

5. Summary and future work

In this paper, the verification benchmark of the field line tracing code NEMATO [14] against magnetic configurations with either helical or poloidal symmetry is reported. A first application of NEMATO to the study of the conditions for chaos healing in the helical RFP, of interest for the interpretation of experimental observations in the RFX-mod device [2], is then discussed. In this stage, we avoid dealing with the uncertainties which may affect the magnetic field reconstruction from experimental measurements, and make use of the magnetic field provided by a 3D visco-resistive MHD simulation of the SPECYL code [3]. We consider a simplified QSH case whose dynamics is characterized by the presence of (nearly) only one secondary mode along with the QSH dominant mode. Nevertheless, the observed evolution of the magnetic field topology is quite rich. It is shown that the magnetic chaos produced after the overlap of the magnetic islands associated with the two relevant MHD modes gets healed in a rather short time around the expulsion of the separatrix of the dominant mode's island. The theoretical picture of chaos healing by separatrix disappearance [9] is thus confirmed. In addition, we show that the chaos reduction begins shortly before the separatrix expulsion, when the first conserved surfaces appear within the chaotic region. The position of the conserved layer corresponds to the values of the helical flux function, computed by assuming the helical symmetry of the dominant mode, where the shear of the safety factor q is reversed with respect to the surrounding chaotic region. The

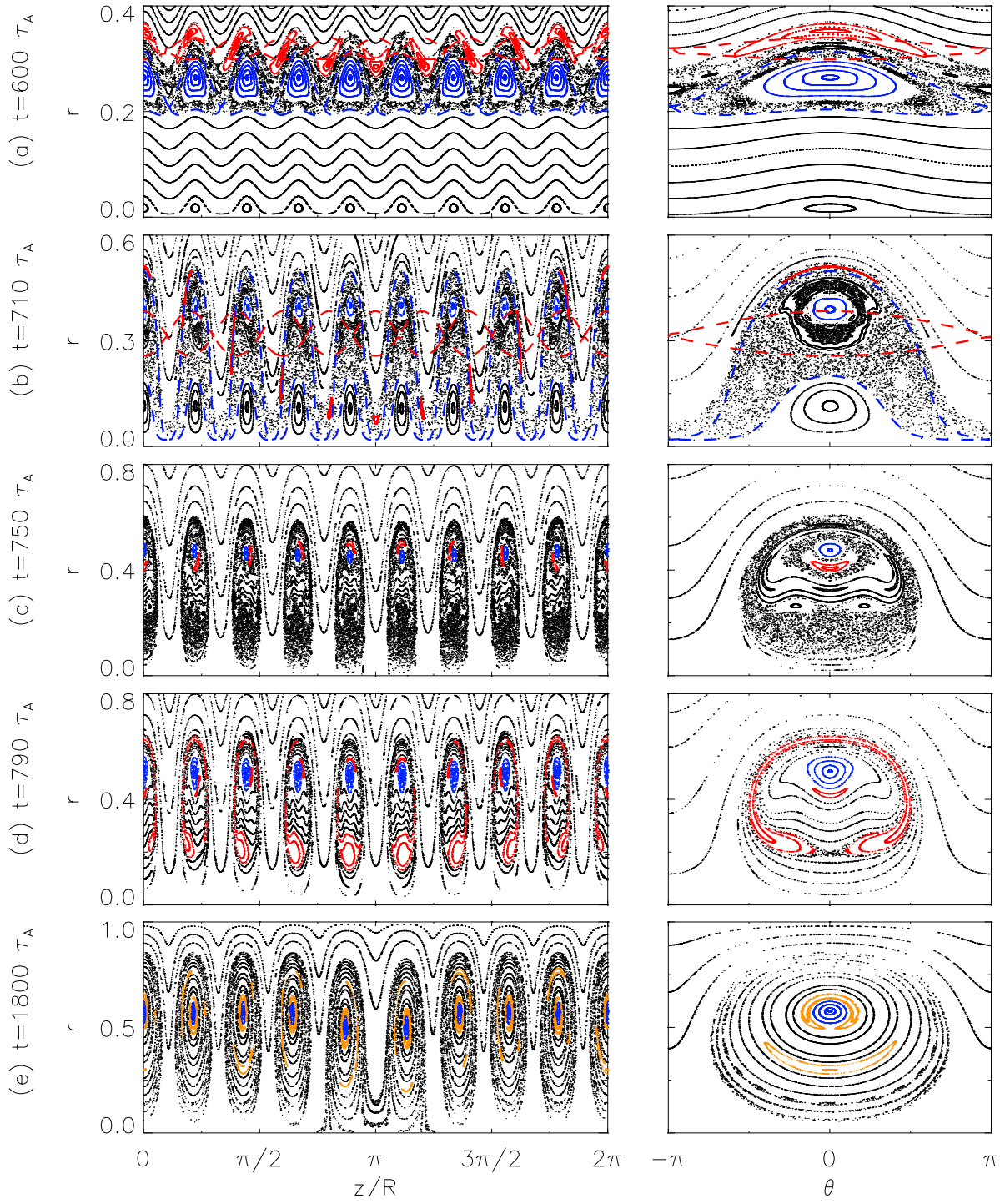

Figure 4. NEMATO simulations for the study of the chaos healing effect in the RFP. Poincaré maps on the $\theta = 0$ plane (first column) and on the $z = 0$ plane (second column) are reported in panels (a-e) for the selected simulation times. Conserved surfaces corresponding to the region close to the $n = -9$ helical axis and to the $n = -10$ magnetic island are shown in blue and red, respectively. The same colors are used in the first two times for dashed curves marking the magnetic separatrices of the two modes, computed from the related helical flux functions.

width of conserved layer increases in time in accordance with the broadening of the reversed shear region. Eventually, after the separatrix disappearance, chaos is completely disappeared from the whole domain, regardless of the shape of the q profile.

Further work is needed to assess the robustness of the described phenomenology in more general QSH conditions. In particular, while the favourable effect of the separatrix expulsion appears to be a robust result, the role played by the magnetic shear, though suggestive of a relation with the experimental observations in the RFX-mod device [10, 11], needs to be interpreted and confirmed. A future detailed study of the conditions for chaos healing in the helical RFP should include, for example, the effect of the following factors: the MHD dynamics (e.g., spontaneous [2] vs. stimulated [19] separatrix expulsion), the shape of the q profile and its shear [20, 21], the number and the amplitude of the secondary modes and of the dominant one, and the geometry (i.e., cylindrical vs. toroidal [22]) of the plasma domain. The use of NEMATO to study the relation between magnetic topology and flow is also envisioned, with reference to both the helical RFP, where a sheared plasma flow could be important for the ITB sustainment [12], and the $m = 0$ island chain located at the reversal surface of the RFP [8]. The latter study turns out to be of interest in relation with the density limit issue in the RFP [23].

Acknowledgments

The authors would like to thank D. F. Escande and F. Sattin for helpful discussions in the course of this study. This work was supported by the European Communities under the Contract of Association between EURATOM/ENEA.

References

[1] Martin P *et al.* 2003 *Nucl. Fusion* **43** 1855
[2] Lorenzini R *et al.* 2009 *Nature Phys.* **5** 570
[3] Cappello S and Biskamp D 1996 *Nuclear Fusion* **36** 571
[4] Cappello S 2004 *Plasma Phys. Control. Fusion* **46** B313
[5] Cappello S and Paccagnella R 1992 *Phys. Fluids B* **4** 611
[6] Finn J M, Nebel R and Bathke C 1992 *Phys. Fluids B* **4** 1262
[7] Cappello S and Escande D F 2000 *Phys. Rev. Lett.* **85** 3838
[8] Spizzo G *et al.* 2006 *Phys. Rev. Lett.* **96** 025001
[9] Escande D F, Paccagnella R, Cappello S, Marchetto C and D'Angelo F 2000 *Phys. Rev. Lett.* **85** 3169
[10] Puiatti M E *et al.* 2009 *Plasma Phys. Control. Fusion* **51** 124031
[11] Gobbin M *et al.* 2010 Vanishing magnetic shear and electron transport barriers in the RFX-mod reversed field pinch *submitted to Phys. Rev. Lett.*
[12] Bonomo F *et al.* 2010 *Proc. 37th EPS Conf. on Plasma Physics, 21-25 June 2010, Dublin* p O2.101
[13] Sattin F *et al.* 2010 Microturbulence studies in RFX-mod *This conference*
[14] Finn J M and Chacón L 2005 *Phys. Plasmas* **12** 054503
[15] Hindmarsh A C 1983 ODEPACK, a systematized collection of ODE solvers *Scientific Computing* ed Stepleman R S (Amsterdam: North-Holland) pp 55–64
[16] Momo B *et al.* 2010 *Proc. 37th EPS Conf. on Plasma Physics, 21-25 June 2010, Dublin* p P4.147
[17] Chirikov B 1979 *Phys. Rep.* **52** 263
[18] Note that, at $t = 750\ \tau_A$, the $n = -10$ islands can only be counted 9 times in the $\theta = 0$ Poincaré surface of Fig. 4(c), instead of the expected 10. This is because the $n = -10$ island (in red) is in fact precessing around the $n = -9$ helical axis (in blue) with a precessing number of 1. The expected winding number of the $n = -10$ island (10) results by adding its strobing number with respect to the Poincaré surface (9) plus the precessing number around the $n = -9$ helical axis (1).
[19] Lorenzini R *et al.* 2008 *Phys. Rev. Lett.* **101** 025005
[20] del-Castillo-Negrete D, Greene J M and Morrison P J 1996 *Physica D* **91** 1
[21] Nasi L and Firpo M C 2009 *Plasma Phys. Control. Fusion* **51** 045006
[22] Sovinec C R *et al.* 2003 *Phys. Plasmas* **10** 1727
[23] Spizzo G *et al.* 2009 *Plasma Phys. Control. Fusion* **52**